

Review Article

Sierpiński-like carpets

Thor Martinsen ¹, Beny Neta ^{1*} and Maital Neta ²

¹Department of Applied Mathematics Naval Postgraduate School, Monterey, CA 93943.

²Department of Psychology University of Nebraska, Lincoln, NE, USA.

*Corresponding author: byneta@gmail.com

Article Info

Keywords: *Nonlinear Equations, Simple Roots, Basins of Attraction, Chaos, Sierpiński carpet, Art.*

Received: 30.09.2025

Accepted: 10.11.2025

Published: 28.11.2025

Abstract

The Sierpiński carpet was developed as a two-dimension extension of the Cantor set. Here we discuss the artistic expression of such carpets along with the development of more visually pleasing Sierpiński-like carpets created by using the basins of attraction of iterative methods for the solution of certain nonlinear equations.

 © 2025 by the author's. The terms and conditions of the Creative Commons Attribution (CC BY) license apply to this open access article.

1. Introduction

In the beginning of the twentieth century the Polish mathematician Waclaw Sierpiński created several fantastic fractals that bear his name. The first, and perhaps most well-known, is the Sierpiński triangle. There are several ways to construct this fractal. One straight-forward way of doing so is to begin with an equilateral triangle. This triangle is then subdivided into four congruent smaller triangles. The center of these triangles is then removed, and the process gets repeated on the remaining three triangles. An example of a Sierpiński triangle created using 6 iterations is provided in Figure 1. The image was generated using the following online programme: Sierpinski Triangle Generator — Free Online Fractal Pattern Creator.

Although Sierpiński first described this triangle in 1915, these triangles appeared on the floors of churches in Rome dating from the 11th century and can also be found in 13th century Cosmati mosaics in the cathedral of Agni in Italy [1, 2].

Another interesting fractal is the Sierpiński carpet, see [3]. It is a generalization of Cantor "third middle" (ternary) set. For Set Theory, see [4–8]. The Cantor ternary set can be described as follows: Start with an interval $[0, 1]$ and divide it to 3 equal part. Remove the middle third (hence the name) and repeat the process on the two thirds left and so on. To create the Sierpiński carpet one starts with a square and divides it to 9 equal squares by using equidistant lines parallel to the edges. Next remove the middle square and repeat the process on the remaining eight squares and so on. The part of the carpet that was not removed at step n has an area of $(8/9)^n$. In Figure 3 we give the Sierpiński carpet created by D.L. Molineu.

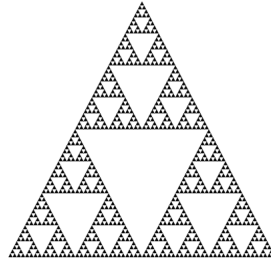


Figure 1: Sierpinski triangle.



Figure 2: 13th century mosaic in Basilica of Santa Maria in Trastevere Rome.

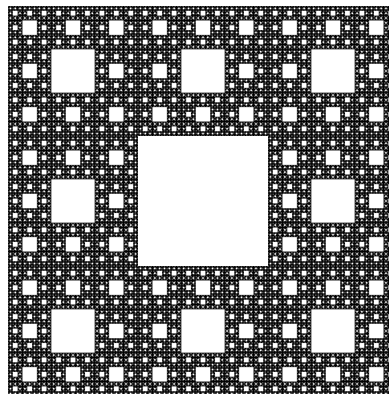


Figure 3: Sierpinski carpet.

Using the Sierpiński carpet as inspiration, we introduce several iterative methods originally used to solve a single nonlinear equation, see [9] and the more recent book [10], that can be plotted and in turn give rise to complex and beautiful carpets in their own right. In the next section we review some iterative methods for the solution of a single nonlinear equation and the idea of basins of attraction, see [11–14].

2. Nonlinear Solvers and Basins of attraction

The solution to a single nonlinear equation,

$$f(x) = 0, \quad (1)$$

can be found in applied science and engineering.

Most numerical solution methods are based on Newton's scheme; i.e., starting with an initial guess x_0 for the root ξ , we create a sequence $\{x_n\}$:

$$x_{n+1} = x_n - \frac{f(x_n)}{f'(x_n)}. \quad (2)$$

The convergence is quadratic, that is,

$$|x_{n+1} - \xi| \leq C_2 |x_n - \xi|^2. \quad (3)$$

To increase the order of convergence, p , one has to include higher derivatives, such as in Halley's scheme [15] or Neta [16], using first and second derivatives to achieve cubic convergence. In order to avoid higher derivatives, one can use multipoint methods; see [9, 10]. Methods can be compared by using efficiency, E , defined as

$$E = p/d, \quad (4)$$

or efficiency index, I , defined as

$$I = p^{1/d}, \tag{5}$$

where d is the number of function (and derivative) evaluations per iteration step.

Recently, the idea of basins of attraction was introduced as a method to quantitatively and qualitatively compare the performance of nonlinear solvers, see [11]. For a given example, one takes a rectangular domain containing the roots and use points in the domain as initial guess of the iterative method. The point is assigned a particular color depending on the root to which the method converged to. If the method did not converge to a root within a certain number of iterations, then the point is rendered black. For example, if we run Newton’s method to find the roots of the complex polynomial $z^2 - 1$, then the domain containing the roots ± 1 will be divided into two rectangles separated by the y -axis. Each rectangle will have a different color, see Figure 4 left. Notice that the basins are not the same if we take the non-polynomial equation $(e^{z+1} - 1)(z - 1)$ having the exact same roots (see Figure 4 right). The root $z = -1$ resulting from the factor containing exponential has stronger pull. Notice also that the basin for $z = 1$ is broken into several disjointed parts.

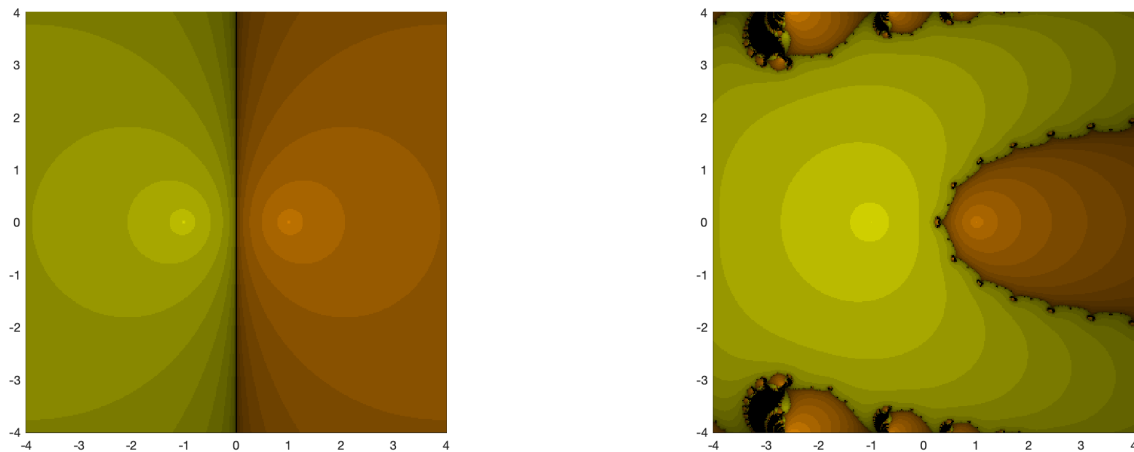


Figure 4: Basins of attraction for Newton’s method of $z^2 - 1$ (left) and the exponential function (right).

3. Steps in creation of carpets

Using Newton’s method (2) we now demonstrate the effect of changing the maximum number of iterations allowed (M). In Figures 5-7, we plot the basins of Newton’s method applied to the polynomial

$$p_2(z) = z^9 + 3z^5 - 4z. \tag{6}$$

using $M = 2, 3, 5, 7, 10$. We choose the following colors for the nine roots of the polynomial starting at the top ($z = +i$) and going counterclockwise to $z = (1 + i)/\sqrt{2}$ and lastly to the center ($z = 0$) the colors are: purple, red, yellow, orange, green, cyan, blue, magenta and light blue.

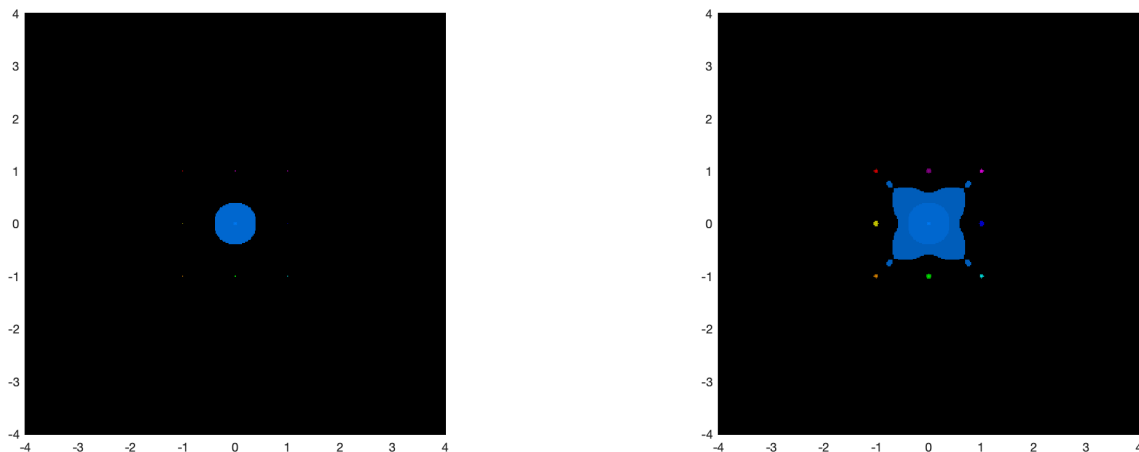


Figure 5: Basins of attraction for Newton’s method for $p_2(z)$ and using $M = 2$ (left) and $M = 3$ (Right)

It is clear from Figure 5 that the root at the center is super attractive. Only points very close to zero are converging to zero in 1 iteration ($M = 2$). Once we increase the number of iterations allowed to 3, we find colored dots (very small basins) where the other roots are (see Figure 5 right). To calculate the percentage of the black area, we count the number of points that lead to divergence versus the total number of points used in the 8 by 8 square (in our case, we have used a total of 160,801). For $M = 2$ we have 99.99% black, For $M = 3$ we have 99.21% down to 95.09% for $M = 5$ (Figure 6 left) and to 90.47% for $M = 7$ (Figure 6 right) and 79.02% for $M = 10$ (Figure 7). Once we use $M = 40$, we have only 0.02% black points. Not all methods will have black points when $M = 40$. We will see later (Figure 9 bottom) that Neta's method (7) has no black point when $M = 40$.

Remark Notice how the basins for the root at the center extends to separate the basins of the other roots.

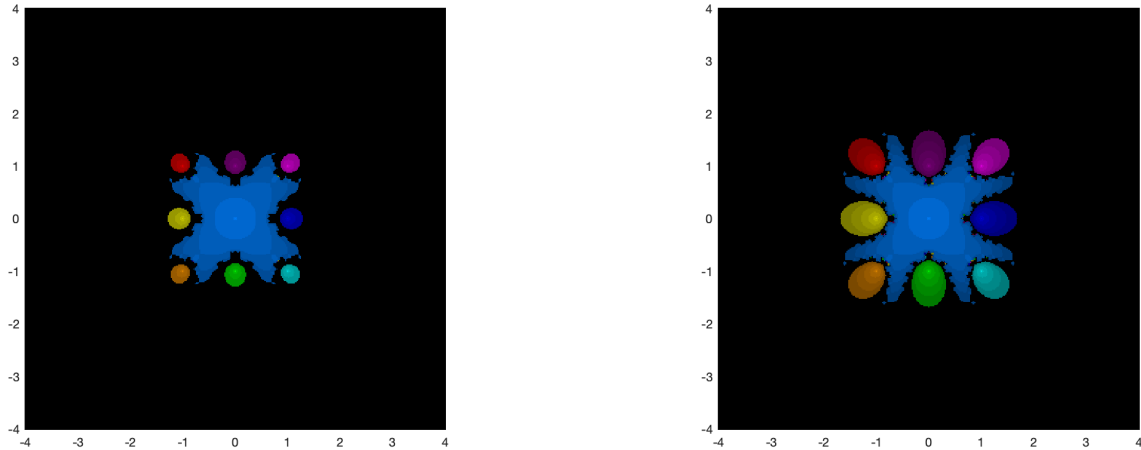


Figure 6: Basins of attraction for Newton's method for $p_2(z)$ and using $M = 5$ (left) and $M = 7$ (right).

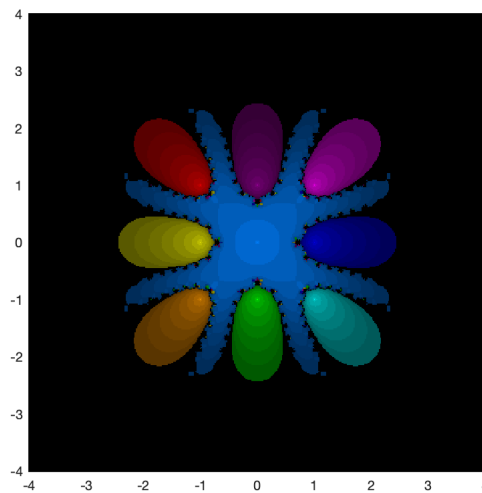


Figure 7: Basins of attraction for Newton's method for $p_2(z)$ and using $M = 10$.

4. The methods to consider

We will consider several methods of various orders of convergence. The first one is Newton's method (2). The second is a third order method due to Neta [13, 16]

$$x_{n+1} = x_n - u_n - A_n \frac{u_n(u_n A_n - 1)}{(-1 + 2u_n A_n)^2}, \quad (7)$$

where

$$u_n = \frac{f(x_n)}{f'(x_n)}, \quad (8)$$

and

$$A_n = \frac{f''(x_n)}{2f'(x_n)}.$$

The third method is of order eight, see [17],

$$\begin{aligned}
 y_n &= x_n - u_n, \\
 z_n &= y_n - \frac{f(y_n)}{2f[y_n, x_n] - f'(x_n)}, \\
 x_{n+1} &= z_n - \frac{f[z_n, y_n]}{f[z_n, x_n]} \frac{f(z_n)}{2f[z_n, y_n] - f[z_n, x_n]},
 \end{aligned}
 \tag{9}$$

where the divided differences

$$f[p, q] = \frac{f(p) - f(q)}{p - q}.$$

The last method is a member of family of multistep methods of order 16 due to [18]

$$\begin{aligned}
 y_n &= x_n - u_n, \\
 z_n &= y_n - Q(s_n) \frac{f(y_n)}{f'(x_n)}, \\
 w_n &= z_n - K(s_n, t_n) \frac{f(z_n)}{f'(x_n)}, \\
 x_{n+1} &= w_n - J(s_n, u_n, v_n) \frac{f(w_n)}{f'(x_n)},
 \end{aligned}
 \tag{10}$$

where u_n is given in (8), s_n, t_n and v_n are given by

$$\begin{aligned}
 s_n &= \frac{f(y_n)}{f(x_n)}, \\
 t_n &= \frac{f(z_n)}{f(y_n)}, \\
 v_n &= \frac{f(w_n)}{f(z_n)},
 \end{aligned}
 \tag{11}$$

and

$$\begin{aligned}
 Q(s) &= \frac{1}{1-2s}, \\
 K(s, u) &= \frac{(-1+s)^2}{(1-2s)(1-2s-u+2s^2u)}, \\
 D_1(s, u, v) &= (-1+2s)(1-u+2s(-1+su))((1-2s)(-1+2s+u-2s^2u)^2 \\
 &\quad +((-1+2s)^3 - (1-2s)^2(-1+3s^2)u - (-1+2s)(1+2s(-2+(-2+s)^2s))u^2 \\
 &\quad +(-1+s)(1+s(-3+2s(1+s)(2+s(-4+3s))))u^3)v), \\
 J(s, u, v) &= -((-1+s)^2(1-2s+(-1+s+s^2)u)^2(1+3s^2+u-2s(1+u)))/D_1(s, u, v).
 \end{aligned}$$

5. Results

We now plot the basins for the above methods for two examples of polynomials of degree 9.

$$p_1(z) = z^9 - z \tag{12}$$

and

$$p_2(z) = z^9 + 3z^5 - 4z. \tag{13}$$

Eight of the roots of $p_1(z)$ are equally spaced on a circle of radius 1 and the ninth is at the center of the circle. The roots of $p_2(z)$ are at the vertices of a 2 by 2 square centered at the origin, 4 more are the mid points of the edges and the ninth at the center of the square. The difference is that the roots of $p_2(z)$ on the vertices of the square are outside the circle of roots of $p_1(z)$. We use a maximum of 40 iterations before declaring a point is black (divergent sequence started at that point). We stop the iteration when the latest iterate is close to a root with 10^{-7} accuracy. Clearly we can adjust these two parameters to affect the Sierpiński-like carpet analogously to stopping the process when creating a Sierpiński carpet.

In Figure 8, we display the Sierpiński-like carpet created using Newton’s method. As we mentioned before, the root at the center has a larger pull and so its basin stretches in between the other basins. To an observer this perhaps brings to mind rainbow colored sunbeams emanating from a stained glass window.

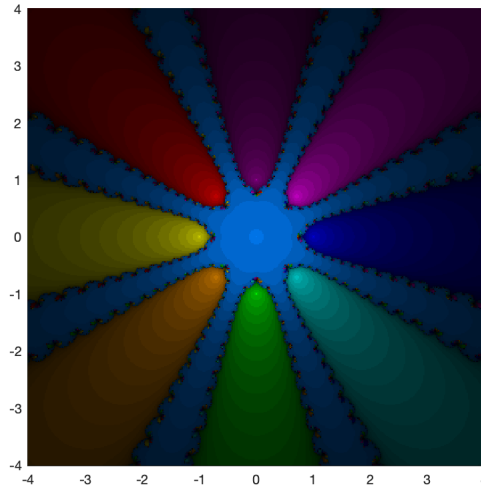


Figure 8: Basins of attraction for Newton's method for $z^9 - z$.

In Figure 9 we plotted the basins for the same roots using the method Neta31, given by (7). This produces a veritable kaleidoscope of colors. One might be tempted to call it organized chaos. The blue center is surrounded by concentric multi-colored necklaces of the other basins. Notice that the order of the colored pearls in each necklace is identical, however, the outer necklace is a 180 degree rotation of the inner necklace. This pattern repeats. In order to see this clearly, we have ran the same method on the same square using one million points instead of 160,801 points. Figure 10 shows the basins. We have also zoomed to the 2 by 2 square centered at the origin to see better what is going on in Figure 11. Now one could discover additional concentric necklaces, the orientation of which agreed for every other necklace. The keen observe will further notice that slightly outside the radius of a given necklace, smaller necklaces appear between each successive pair of pearls. Within the confines of these smaller necklaces yet smaller necklaces appear, seemingly spiraling down into a dark abyss where the image resolution obscures any further detail.

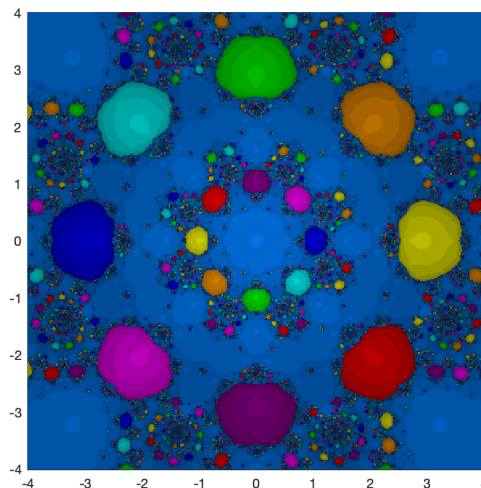


Figure 9: Basins of attraction for the Neta31 method for $z^9 - z$.

In Figure 12 and Figure 13 we show the basins for the same methods for $p_2(z)$. The Figure 12 plot for Newton's method is almost identical to the previous one. However, the Figure 13 plot, albeit also an intricate kaleidoscope of shapes and colors, is slightly different. The center "necklace" has now become a square of 8 basins. This square is surrounded by a larger circle of 8 basins. However, here only 4 of the 8 colored basins are present. Each of these eight basins appear in side-by-side pairs of the same colors, namely yellow, green, blue, and burgundy. The 4 missing orange, turquoise, purple, and red basins now appear farther out in the corners of the carpet. Although the concentric structures are now alternating between being squares and circles, similar colors in successive "necklaces" do follow the previous pattern of being 180 degree rotations of one another.

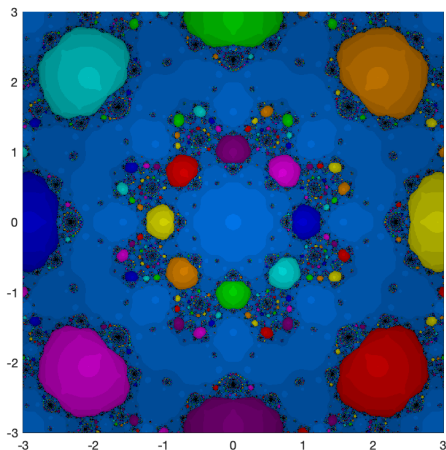


Figure 10: Basins of attraction for the Neta31 method for $z^9 - z$ Using 1 million points.

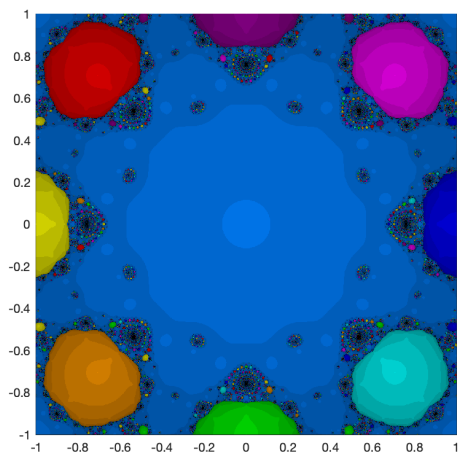


Figure 11: Basins of attraction for the Neta31 method for $z^9 - z$ zooming on the center 2 by 2 square.

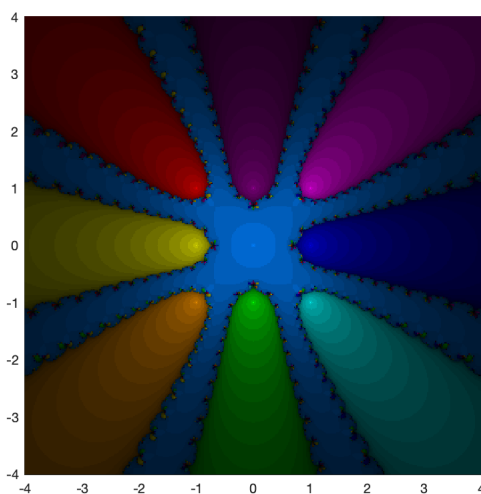


Figure 12: Basins of attraction for Newton's method for $z^9 + 3z^5 - 4z$.

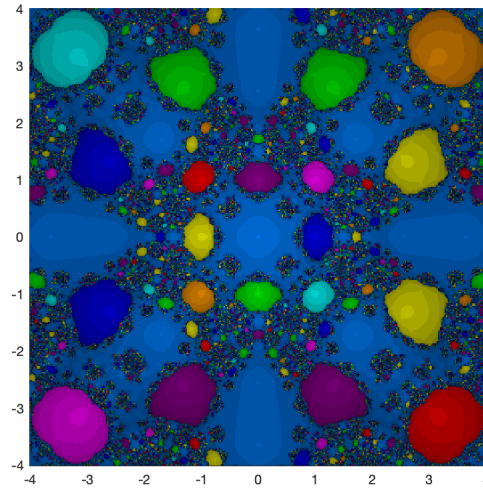


Figure 13: Basins of attraction for the Neta31 method for $z^9 + 3z^5 - 4z$.

The plots of the basins for the eighth order method due to [17] are given in Figure 14 and Figure 15. Now the blue rays emanating from the origin appear broken by the jagged edges of the other colored rays. These two images may perhaps appear to an observer as if they are looking up at a blue sky surrounded by a forest of multi-colored pine trees.

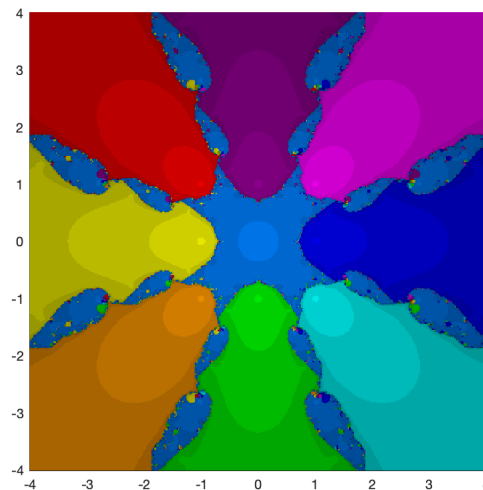


Figure 14: Basins of attraction for Sharma and Arora's eighth order method for $z^9 + 3z^5 - 4z$.

In Figure 16 and Figure 17 we present the basins for the method of order 16 due to [18]. Here the order of the pearls on the inner square is the same as the order on the outer square. In between those two there is a blue belt (part of the basin of the root at the center) with many small pearls of various colors.

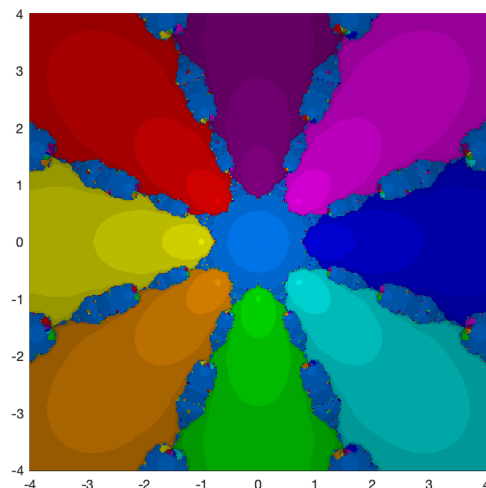


Figure 15: Basins of attraction for Sharma and Arora's eighth order method for $z^9 - z$.

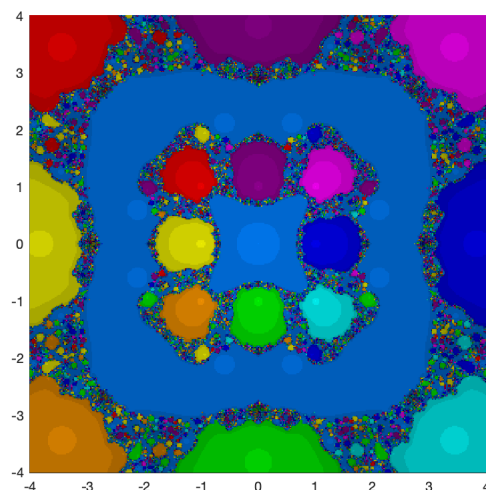


Figure 16: Basins of attraction for Sharma et al. method for $z^9 + 3z^5 - 4z$.

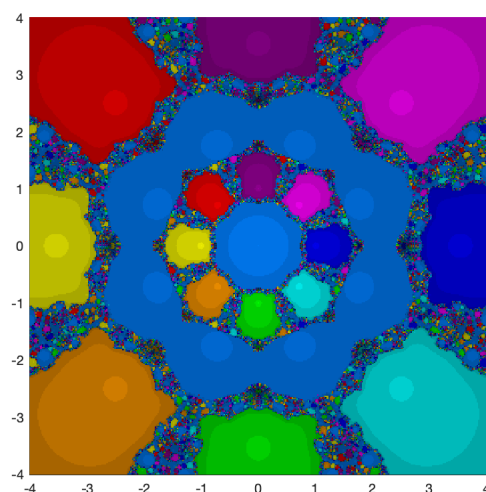


Figure 17: Basins of attraction for Sharma et al. method for $z^9 - z$.

6. Artistic discussion

Sierpiński carpet, see Figure 3 can be viewed as an art deco design. Even if we change the colors of the removed squares at each iteration, the appearance of the carpet do not change significantly. See Figure 18.

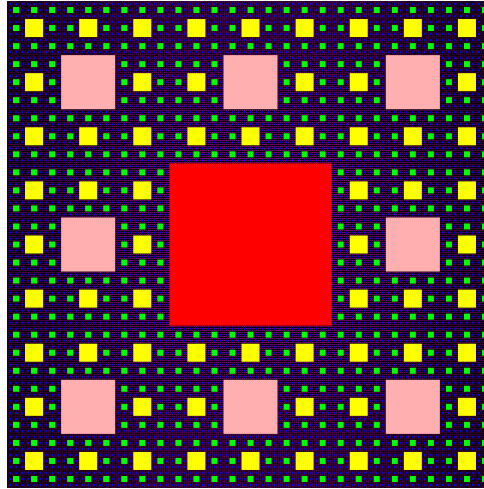


Figure 18: Sierpinski carpet in color

The Sierpiński-like carpets we have created, in particular those created using the Neta31 iterative solver, see Figures 9 and 13, are more intricate. Their circular designs share similarities with very old art and architecture as well as modern science-inspired artistic creations. For some, these carpets may remind observers of Gothic stained glass rose windows, such as those found in the Notre Dame or Chartres cathedrals in France. See for example Figure 19 (left) from [19]. Others may see similarities with cymatics visualization of sound such as Laurent Lettrée’s art created by resonating water with sound. See 19 (right) from [20]. For more on cymatics see [21].

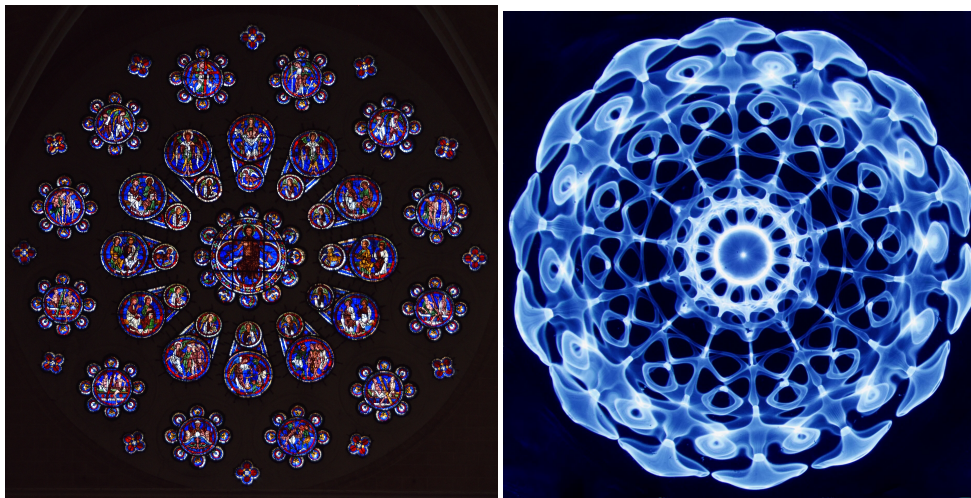


Figure 19: West rose window, Chartres cathedral (left) and cymatics art by Laurent Lettrée created by resonating water with sound (right).

The Sierpiński-like carpet in Figure 9 shows a relatively strong sense of balance and symmetry. Circular patterns are processed more easily (Gestalt) and convey features of harmony and are thus more pleasing and easier on the eyes than the one in Figure 13, see Bar and Neta and other works by, [22]. On Figure 13 there is symmetry albeit less obvious and seems sharper and thus harder on the eyes. The method due to [18] also creates some intricate designs (see Figures 16-17) but not as organized as the one by Neta31. There is some similarity to the radial shapes created by Newton’s method (Figure 8). These are more abstract art and could also link to Gestalt principles. Notice the difference between Figures 16 and 17. The first is square and the latter starts with a circle going to a flower. Again the curves are more pleasing than the edges.

7. Conclusions

Inspired by the work of Sierpiński we enlisted the help of iterative nonlinear equation solvers and basins of attraction to create fascinating sierpiński-like carpets. Although low order algorithms, such as Newton’s method, often are more stable and therefore preferable from a computational perspective, higher order methods such as those attributed to Neta and Sharma are, artistically speaking, more pleasing. These methods produce extremely complex and beautiful structures that exhibit self-similarity at different scales. In an analogous way to Sierpiński carpets, these new carpets become more complex and reveal increasing amounts of structure with increasing numbers of iterations.

Article Information

Disclaimer (Artificial Intelligence): The author(s) hereby declare that NO generative AI technologies such as Large Language Models (ChatGPT, COPILOT, etc.), and text-to-image generators have been used during writing or editing of manuscripts.

Competing Interests: Authors have declared that no competing interests exist.

References

- [1] L. Tedeschini-Lalli and L. E. Conversano. Sierpinski Triangles in Stone on Medieval Floors in Rome. *Aplimat- Journal of Applied Mathematics*, 4(4):113–122, 2011.
- [2] P. Brunori, P. Magrone, and L. Tedeschini-Lalli. Imperial porphyry and golden leaf: Sierpinski triangle in a medieval cloister. In L. Cocchiarella, editor, *ICGG 2018-Proceedings of the 18th International Conference on Geometry and Graphics. ICGG 218. Advances in Intelligent Systems and Computing, vol 809*, Cham, 2019. Springer.
- [3] W. F. Sierpinski. Sur une courbe cantorienne qui contient une image biunivoque et continue de tout courbe donnée. *C. R. Acad. Sci. Paris*, 162:629–632, 1916.
- [4] J. P. Mayberry. *The Foundations of Mathematics in the Theory of Sets*. Cambridge University Press, Cambridge, U. K, 2000.
- [5] H. J. S. Smith. On the integration of discontinuous functions. In *Proc. London Math. Soc. First Series*, 6, pages 140–153, 1874.
- [6] P. du Bois-Reymond. Der Beweis des Fundamentalsatzes der Integralrechnung. *Math. Anal.*, 16:115–128, 1880.
- [7] P. W. Zehna and R. L. Johnson. *Elements of Set Theory, Allyn and Bacon Inc.* Boston, 1967.
- [8] G. Cantor. Über unendliche, lineare Punktmannigfaltigkeiten V. *Math. Ann.*, 21:545–591, 1883.
- [9] J. F. Traub. *Iterative Methods for the Solution of Equations*. Prentice Hall, New York, NY, USA, 1964.
- [10] M.S. Petković, B Neta, L.D. Petković, and J. Džunić. *Multipoint Methods for the Solution of Nonlinear Equations*. Amsterdam, The Netherlands, Elsevier, 2012.
- [11] B. D. Stewart. Attractor basins of various root-finding methods. Master’s thesis, Naval Postgraduate School, Department of Applied Mathematics, Monterey, CA, USA, 2001.
- [12] C. Chun and B. Neta. Comparative study of methods of various orders for finding simple roots of nonlinear equations. *Journal of Applied Analysis and Computation*, 9:400–427, 2019.
- [13] B. Neta. Dynamics of some one-point third-order methods for finding simple roots of nonlinear equations. *Comm. Numer. Anal.*, 2: 111–130, 2018.
- [14] G. Irving and H. Segerman. Developing fractal curves. *J. Math. and the Arts*, 7:103–121, 2013.
- [15] E. Halley. A new, exact and easy method of finding the roots of equations generally and that without any previous reduction. *Philos. Trans. R. Soc. Lond.*, 18:136–148, 1694.
- [16] B. Neta. Several New Methods for Solving Equations. *International J. Computer Mathematics*, 23:265–282, 1988.
- [17] J. R. Sharma and H. Arora. A new family of optimal eighth order methods with dynamics for nonlinear equations. *Appl. Math. Comput.*, 273:924–933, 2016.
- [18] J. R. Sharma, I. K. Argyros, and D. Kumar. On a general class of optimal order multipoint methods for solving nonlinear equations. *J. Math. Anal. Appl.*, 449:994–1014, 2017.
- [19] Ludvig and Wikimedia Commons. Western rose stained glass window, Chartres cathedral, France . 2024. URL https://commons.wikimedia.org/wiki/File:Chartres_Notre-Dame_Windows143_018_2885.jpg. Retrieved June 20, 2025.
- [20] S. Shan and Wikimedia Commons. Cymantic art by Laurent Lettrée by resonating water by sound. 2022. URL <https://commons.wikimedia.org/wiki/File:Cymatic.jpg>. Retrieved June 19, 2025.
- [21] H. Jenny. *Cymatics : A study of wave phenomena and vibration*. Macromedia, Edinburgh, 2007.
- [22] O. Vartanian, G. Navarrote, A. Chatterjee, L. B. Fich, H. Leder, C. Modorn˜o, M. Nadal, N. Rostrup, and M. Skov. Impact of contour on aesthetic judgments and approach-avoidance decisions in architecture. *Proc. National Acad. Sci.*, 110, suppl. 2:10446–10453, 2013.